



Contents lists available at ScienceDirect

# Spectrochimica Acta Part A: Molecular and Biomolecular Spectroscopy

journal homepage: [www.elsevier.com/locate/saa](http://www.elsevier.com/locate/saa)

## Triazole based ratiometric fluorescent probe for Zn<sup>2+</sup> and its application in bioimaging



Murugan Iniya<sup>a</sup>, Dharmaraj Jeyanthi<sup>a</sup>, Karupppiah Krishnaveni<sup>a</sup>, Ayyavu Mahesh<sup>b</sup>  
Duraisamy Chellappa<sup>a,\*</sup>

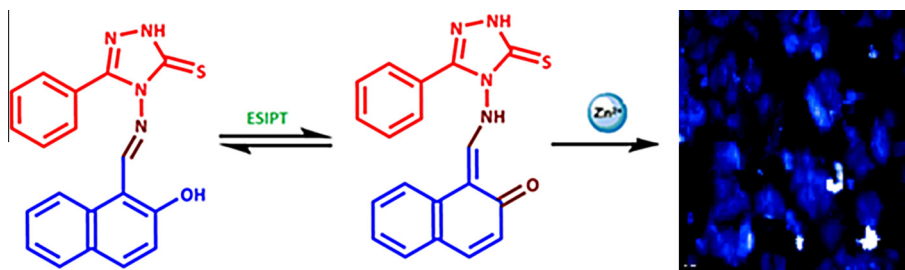
<sup>a</sup>School of Chemistry, Madurai Kamaraj University, Madurai 625021, Tamilnadu, India

<sup>b</sup>School of Biological Sciences, Madurai Kamaraj University, Madurai 625021, Tamilnadu, India

### HIGHLIGHTS

- Triazole based ratiometric fluorescent sensor for Zn<sup>2+</sup> was designed based on ESIPT mechanism.
- The probe displays long excitation wavelength and potential to quantify the concentration of Zn<sup>2+</sup>.
- High stability and cell-permeability is an additional feature of probe.
- The probe is applied successfully for recognizing intracellular Zn<sup>2+</sup> within living cells.

### GRAPHICAL ABSTRACT



### ARTICLE INFO

#### Article history:

Received 5 July 2013

Received in revised form 12 September 2013

2013

Accepted 26 September 2013

Available online 14 October 2013

#### Keywords:

ESIPT

Triazole

Fluorescent sensing

Zinc

Bioimaging

### ABSTRACT

An efficient fluorescent chemosensor 4-((2-hydroxynaphthalen-1-yl)methyleneamino)-3-phenyl-1H-1,2,4-triazole-5(4H)-thione, based on triazole has been designed by condensing 2-hydroxy-1-naphthaldehyde with amine, appended to 1,2,4-triazole unit. The probe displays excellent selectivity and sensitivity in both absorbance and fluorescence detection of Zn<sup>2+</sup> over other essential metal ions. The nature of fluorescence behavior of receptor upon addition of Zn<sup>2+</sup> has been obtained from Density Functional Theory calculations. Imaging experiment indicates that probe works effectively for intracellular Zn<sup>2+</sup> imaging with good cell permeability and biocompatibility.

© 2013 Elsevier B.V. All rights reserved.

### Introduction

Zinc is present in numerous enzymes and plays significant role in DNA synthesis, hormone control, enzymatic reactions and cell proliferation [1]. Zn<sup>2+</sup> can mimic the actions of hormones, growth factors and cytokines and so can act as intracellular signaling molecules. It plays vital role in biological processes such as neurotransmission, signal transduction and gene expression [2]. However excessive quantities of Zn<sup>2+</sup> intake may lead to both acute and

chronic toxicity. It is also a causal contributor in both the acute brain injury of stroke, head trauma, seizures or cardiac arrests [3] and the slow and relentless brain injury of the neurodegenerative disorders such as Alzheimer's disease and possibly amyotrophic lateral sclerosis [4]. Therefore, a convenient and rapid method for analysis of Zn<sup>2+</sup> is highly demanded. Among various analytical methods available, fluorescence method stands out as the technique of choice due to its simplicity, cost effectiveness and high sensitivity [5].

Accordingly, several Zn<sup>2+</sup> ion sensing molecules has been developed by various detection mechanisms based on rhodamine spiro-lactam [6], spiropyran [7], pyrazoline [8], fluorescein [9], Pyrene

\* Corresponding author. Tel.: +91 452 2456614; fax: +91 452 2459181.

E-mail address: [dcmku123@gmail.com](mailto:dcmku123@gmail.com) (D. Chellappa).

[10], naphthalic anhydride [11], anthracene [12] and cyclen moiety [13]. Tang et al. reported that dipicolylamine appended quinoline senses  $Zn^{2+}$  over other competing cations, based on chelation enhanced fluorescence [14]. Ferrocenyl seleno unit has been utilized for the fluorescent detection of  $Zn^{2+}$  based on ICT mechanism by Jing et al. [15]. Recently Zhao et al. reported 1,8 naphthalimide containing receptor for  $Zn^{2+}$  and successfully applied it to detect endogenous  $Zn^{2+}$  ions in live cells [16]. Considerable efforts like this have been made towards the design and synthesis of various fluorescent chemo-sensors for the in vitro and in vivo detection of  $Zn^{2+}$ . However most of reported sensors lack either ratiometric response, or bio-compatibility besides suffering from interference of  $Cd^{2+}$  ions. To the best of our knowledge, very few chemosensors satisfying the above-mentioned requirements have been reported. Therefore, the design of simple and easily accessible Zn(II) selective ratiometric chemosensor is still a challenge. Amongst the different photo physical processes, Excited State Intramolecular Proton Transfer (ESIPT) has gained a special status due to unique emission features such as the large Stokes shift and the transient character of ground state of emissive species of ESIPT chromophores (i.e. the keto tautomer) [17]. ESIPT facilitates fluorescence probing of chemicals, bio-molecules, and ions due to its unique spectral sensitivity to environmental medium [18]. The fluorescence of ESIPT chromophores can be perturbed by many intermolecular interactions, such as removal of the hydrogen involved in the ESIPT process, thus paving way for sensing metal ions [19]. Triazolyl-containing compounds especially 1,2,3-triazoles have been employed as fluorescent indicators for metal ions [20] and recently, 1,2,4-triazole moiety has been utilized for electrochemical sensing of Gd(III) ion, and L-tyrosine [21,22]. The derivatives of 1,2,4-triazoles are well known for its wide range of therapeutic properties [23], this work adds a new dimension to the class of 1,2,4-triazoles as an ESIPT based fluorescent sensor for the recognition of  $Zn^{2+}$  over other metal ions with significant increase in fluorescence.

In continuation of our ongoing research for the development of fluorescent chemosensors [24–28], herein, we report the synthesis and photonics of a triazole appended simple fluorescent chemosensor namely 4-((2-hydroxynaphthalen-1-yl)methyleneamino)-3-phenyl-1H-1,2,4-triazole-5(4H)-thione (TZNP). This probe exhibits features such as large Stokes shifted emission, ratiometric response in addition to sensing  $Zn^{2+}$  with high sensitivity and excellent selectivity. Apart from this it has good cell-permeability and bio-compatibility.

## Materials and methods

### General

All the chemicals used were of analytical reagent grade and purchased from Sigma–Aldrich Chemical Company. Solvents used were of HPLC grade unless otherwise stated. Binding properties of metal ion with TZNP were evaluated by chloride salts of metal ions such as  $K^+$ ,  $Na^+$ ,  $Ca^{2+}$ ,  $Fe^{2+}$ ,  $Mg^{2+}$ ,  $Fe^{3+}$ ,  $Ag^+$ ,  $Mn^{2+}$ ,  $Cu^{2+}$ ,  $Co^{2+}$ ,  $Ni^{2+}$ ,  $Cd^{2+}$ ,  $Cr^{3+}$ ,  $Pb^{2+}$  and  $Hg^{2+}$  ions. Metal solutions were prepared with Double distilled water. UV–Vis absorption spectra were recorded using JASCO V-550 spectrophotometer. Fluorescence spectra measurements were performed on a F-4500 Hitachi fluorescence spectrophotometer. The excitation and emission slit width was kept constant at 5 nm.  $^1H$  and  $^{13}C$  NMR spectra were recorded on a Bruker 300 MHz NMR instrument. IR spectra in KBr discs were recorded using JASCO FT-IR Spectrophotometer. Electro-spray Ionisation mass spectral (ESI–MS) analysis was performed in the positive ion mode on a liquid chromatography–ion trap mass spectrometer (LCQ Fleet, Thermo Fisher Instruments Limited, US). Fluorescence quantum yields ( $\Phi_f$ ) were determined with respect to Rhodamine B in ethanol solution ( $\Phi_f = 0.97$ ).

### Synthesis of 4-amino-3-phenyl-1H-1,2,4-triazole-5(4H)-thione (3)

A mixture of methyl benzoate (1.36 ml, 1 mM) and hydrazine hydrate (0.5 ml, 1 mM) was allowed to reflux for 6 h. The total volume of the solution was reduced to half and it was cooled in ice water. The crystals formed were filtered, washed thoroughly with water to yield benzoic acid hydrazide (1). The benzoic acid hydrazide (1.36 g, 1 mM) was treated with alcoholic solution of KOH (0.84 g, 1.5 mM) and carbon disulphide (1.45 ml, 1.5 mM) for 15 h at room temperature with constant stirring. After dilution with anhydrous ether, precipitated potassium 3-benzoyl dithiocarbazine (2) was washed with anhydrous ether and dried under vacuum. To the suspension of potassium 3-benzoyl dithiocarbazine (2.49 g, 1 mM) in water, hydrazine hydrate (1.5 ml, 3 mM) was added and refluxed for 3 h with occasional shaking. It was diluted with water; acidified and resulting solid was filtered, washed thoroughly with water and recrystallized from ethanol to yield (3).  $^1H$  NMR (300 MHz, DMSO- $d_6$ ): 7.7 (m, 5H, Ar-H), 7.9 (s, 2H,  $NH_2$ ), 3.5 (s, 1 H, HN-C). MS (ESI)  $m/z$ : 193 ( $3 + H^+$ )

### Synthesis of 4-((2-hydroxynaphthalen-1-yl)methyleneamino)-3-phenyl-1H-1,2,4-triazole-5(4H)-thione (TZNP)

A mixture of 4-amino-3-phenyl-1H-1,2,4-triazole-5(4H)-thione (1.92 g, 1 mM) (3) and 2-Hydroxy-1-naphthaldehyde (1.72 g, 1 mM) in hot ethanol was treated with concentrated HCl (0.5 ml) and allowed to reflux for 3 h. The solid formed on cooling was filtered, washed with cold ethanol, then dried and recrystallized from ethanol to yield TZNP. Yield, 70%; Anal. Found: C: 65.6, H: 4.1, N: 16.3, S: 9.4. Cal. for: C: 65.4, H: 3.9, N: 16.1, S: 9.2%.  $^1H$  NMR (300 MHz, DMSO- $d_6$ ):  $\delta$  = 6.41–7.91 (m, 11H, ArH), 9.42 (s, 1H, CH=N), 10.4 (s, 1H, OH) and 13.5 (s, 1 H, HN-C);  $^{13}C$  NMR (75 MHz, DMSO- $d_6$ ):  $\delta$  = 166.4, 162.9, 160.6, 148.8, 136.4, 132.2, 131.1, 129.3, 129.1, 129.0, 128.7, 128.4, 125.9, 124.3, 123.8, 118.8, 108.7; MS (ESI)  $m/z$ : 347 (TZNP +  $H^+$ );

### Cation recognition studies and quantum yield calculation

The recognition properties of TZNP towards cations were investigated in DMSO/ $H_2O$  (2:8 v/v) system through UV–Vis and Fluorescence measurements. The solutions of metal ions ( $1 \times 10^{-3}$  mol/L) were prepared in distilled water. A solution of TZNP ( $1 \times 10^{-5}$  mol/L) was made up with DMSO solvent. Different ion solutions were added in portions to TZNP and absorption/fluorescent intensity changes were recorded at room temperature after each addition. The fluorescence quantum yield  $\Phi_s$  was estimated from the absorption and fluorescence spectra of probe according to Eq. (1), where the subscript  $s$  and  $r$  stand for the sample and reference (rhodamine B,  $\Phi_f = 0.97$  in ethanol), respectively.  $\Phi$  is the quantum yields,  $A$  represents the absorbance at the excitation wavelength,  $S$  refers to the integrated emission band areas and  $n_D$  is the solvent refractive index.

$$\Phi_s = \Phi_r \frac{S_s A_r n_{DS}^2}{S_r A_s n_{Dr}^2} \quad (1)$$

### Computational details

Density functional theory (DFT) calculations were performed with 6-31G\* and LANL2DZ basis set using Gaussian 03 program to understand the turn on fluorescence behavior of TZNP on complexation with  $Zn^{2+}$ . The geometries of keto and enol form of TZNP and TZNP- $Zn^{2+}$  were optimized by DFT-B3LYP using 6-31G and LANL2DZ basis sets respectively.

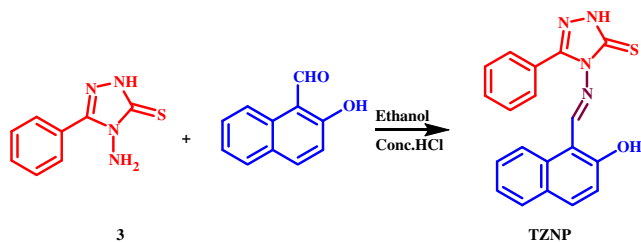
### Cell line and culture condition

MCF-7 cells were obtained from National Center for Cell Science (NCCS), Pune, India. MCF-7 cells were maintained in Minimum Essential Medium (Himedia, India), supplemented with 10% Fetal Bovine Serum (FBS) and antibiotics (100 U/mL of penicillin and 100 g/mL streptomycin, respectively; Himedia, India), sodium bicarbonate (1.5%), sodium pyruvate (1 mM) and non-essential amino acids (1×), Himedia, India and maintained in a humidified incubator at 37 °C with 5% CO<sub>2</sub>.

Localization of TZNP and the ability of TZNP for Zn<sup>2+</sup> recognition were investigated in MCF-7 cell line. Briefly, MCF-7 (7 × 10<sup>3</sup> cells/well) was seeded onto 96 well cell carrier microplates (PerkinElmer, US). When the cells reached 80% confluence, the media were changed. Cells were then treated with 10 μM of TZNP alone and supplemented with Zn<sup>2+</sup> (10 μM) and the plate was incubated for 24 h in humidified incubator at 37 °C with 5% CO<sub>2</sub>. The cells were washed twice with PBS buffer and fluorescence of probe localized in live cells was determined using Operetta High Content Imaging System (PerkinElmer, US).

### Cytotoxicity testing

MCF-7 cells were maintained in a humidified atmosphere containing 5% CO<sub>2</sub> at 37 °C in Minimum Essential Medium (Himedia, India), supplemented with 10% Fetal Bovine Serum (FBS) and antibiotics (100 U/mL of penicillin and 100 g/mL streptomycin, respectively; Himedia, India), sodium bicarbonate (1.5%), sodium pyruvate (1 mM) and non-essential amino acids. Briefly, MCF-7 cells with a density 1 × 10<sup>4</sup> cells per well were precultured into 96-well microtiter plates for 48 h under 5% CO<sub>2</sub>. The probe



Scheme 1. Synthetic route of TZNP.

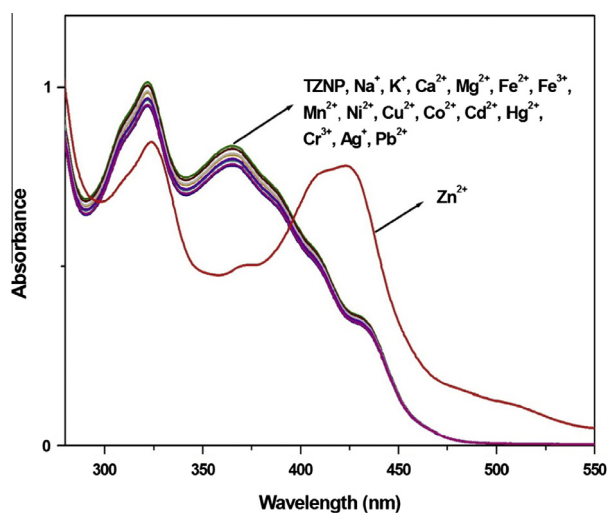


Fig. 1. UV-Vis spectra of TZNP (10 μM) with various cations (1 × 10<sup>-3</sup> M) in DMSO/H<sub>2</sub>O (2:8 v/v) system.

(0–50 μM) was added in micro wells and then incubated in 5% CO<sub>2</sub> at 37 °C, for 1 day. Then each well was loaded with 10 μL MTT [3-(4,5-dimethylthiazol-2-yl)-2,5-diphenyltetrazolium bro-

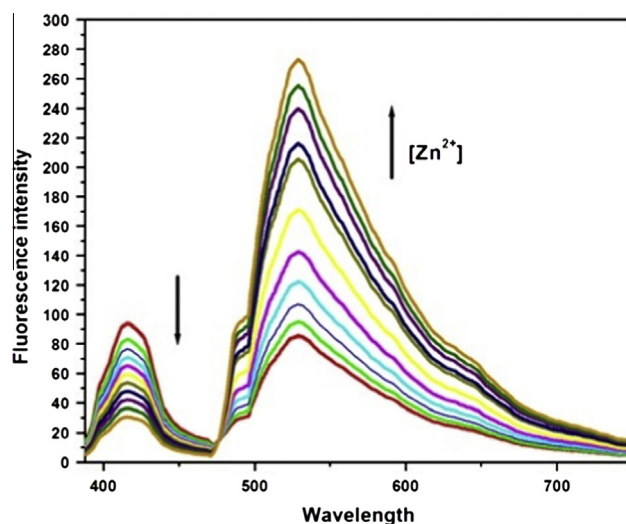
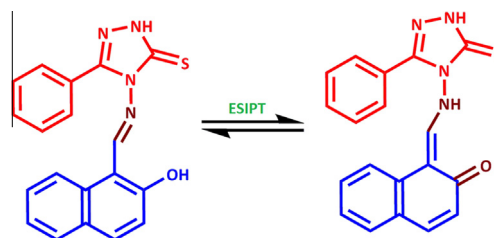


Fig. 2. Changes in emission spectra of TZNP (10 μM) upon gradual addition of Zn<sup>2+</sup> (0–10 μM) in DMSO/H<sub>2</sub>O (2:8 v/v) system. Excitation at 370 nm. Slit width is 5 nm.



Scheme 2. Enol and keto form of TZNP.

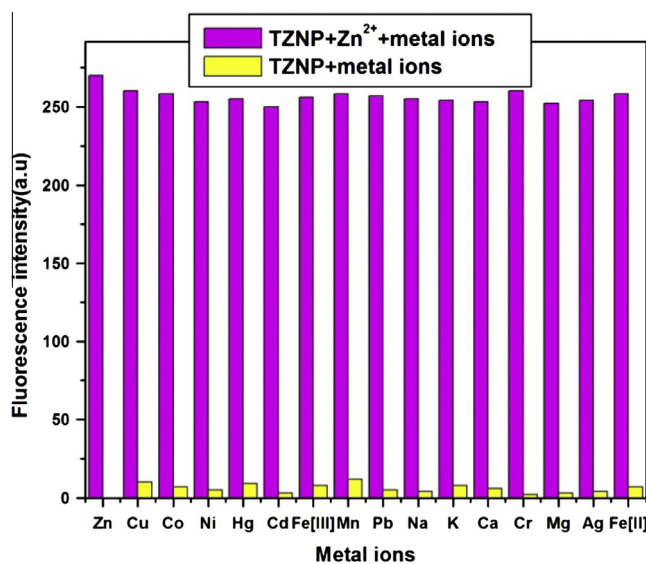


Fig. 3. Competitive fluorescence responses of 1 μM TZNP at 529 nm in the presence of various metal ions including Zinc. Yellow bar represent the addition of various metal ion to TZNP. The violet bar represents the change of emission that occurs upon subsequent addition of Zn<sup>2+</sup> to the above solution. Excitation was provided at 370 nm. Slit width is 5 nm. (For interpretation of the references to color in this figure legend, the reader is referred to the web version of this article.)

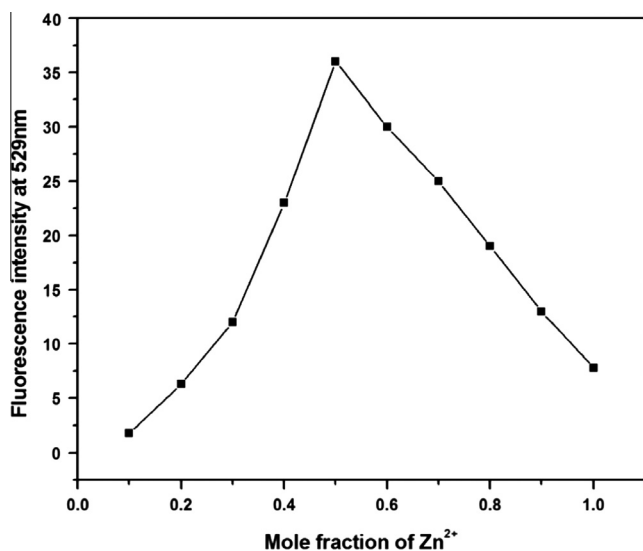


Fig. 4. Job's plot for TZNP and Zn<sup>2+</sup> illustrating the formation of 1:1 (TZNP/Zn<sup>2+</sup>) complex.

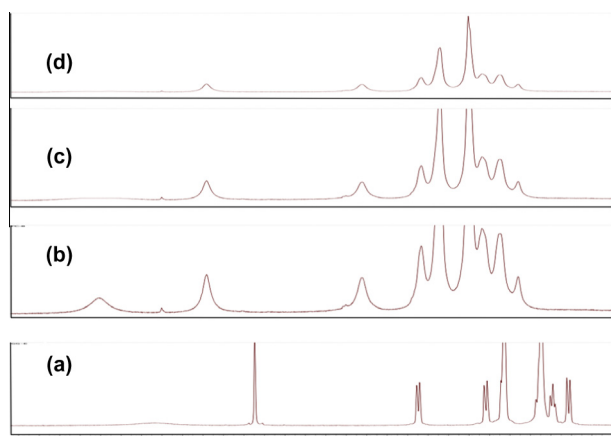


Fig. 5. <sup>1</sup>H NMR spectra of TZNP without and with the addition of Zn<sup>2+</sup> in DMSO-d<sub>6</sub>. (a) TZNP, (b) TZNP + 0.5 eq of Zn<sup>2+</sup>, (c) TZNP + 1 eq of Zn<sup>2+</sup> and (d) TZNP + 1.5 eq of Zn<sup>2+</sup>.

midel] solution (5 mg mL<sup>-1</sup> in PBS pH = 7.4) for 4 h at 37 °C. Medium was subsequently removed from wells and resulting formazan crystals solubilised in 100 μL DMSO. The cell viability was determined by measuring the absorbance of each well at 540 nm using microplate reader. The percentage of cell viability was calculated according to the following equation.

$$\text{Inhibition rate (IR\%)} = \frac{\text{OD (control)} - \text{OD Drug treated cells}}{\text{OD (control)}} \times 100\%$$

## Results and discussion

The starting materials benzoic hydrazide (1), potassium 3-benzoyl dithiocarbazate (2), and 4-amino-3-phenyl-1H-1,2,4-triazole-5(4H)-thione (3) were prepared following known procedure [29] (Scheme – see Supplementary data). The chemosensor TZNP was synthesized by treating 4-amino-3-phenyl-1H-1,2,4-triazole-5(4H)-thione (3) with 2-hydroxy-1-naphthaldehyde in ethanol (Scheme 1) [30]. The structure of TZNP was well characterized by <sup>1</sup>H NMR, <sup>13</sup>C NMR and ESI-MS analysis and given in Supplementary data (Figs. S1–S4).

The cation binding properties of TZNP was investigated by monitoring their absorption and emission spectra upon addition of various metal ions in DMSO/H<sub>2</sub>O (2:8 v/v) system. The absorption spectrum of TZNP exhibited two main bands centered at 322 nm and 367 nm. Addition of 1 equiv of Zn<sup>2+</sup> in the solution of TZNP leads to appearance of new absorption band at 417 nm with the color of solution changing simultaneously to yellowish green (Fig. 1). Under identical conditions, metal ions such as Li<sup>+</sup>, Na<sup>+</sup>, Mg<sup>2+</sup>, K<sup>+</sup>, Ca<sup>2+</sup>, Mn<sup>2+</sup>, Co<sup>2+</sup>, Ni<sup>2+</sup>, Fe<sup>3+</sup>, Cu<sup>2+</sup>, Ag<sup>+</sup>, Cd<sup>2+</sup>, Cr<sup>3+</sup>, Hg<sup>2+</sup> and Pb<sup>2+</sup> failed to behave like Zn<sup>2+</sup>, indicating that TZNP acts as an efficient and selective sensor for Zn<sup>2+</sup> over other essential metal ions tested. To determine the coordinating behavior of TZNP with Zn<sup>2+</sup>, an UV-Vis titration experiment was performed (Fig. S5). The addition of increasing amount of Zn<sup>2+</sup> ions to the solution of TZNP resulted in the appearance of a new band at 417 nm with simultaneous decrease in absorption at 367 nm, generating isobestic points at 381 nm and 434 nm, which indicated the existence of equilibrium between TZNP and TZNP-Zn<sup>2+</sup>.

Chemosensor TZNP which has intramolecular hydrogen bond between the phenolic O–H and nitrogen of imine undergoes ESIPT and yields emission bands at 416 nm and 529 nm with the fluorescence quantum yield value being 0.04, when excited at 370 nm in the absence of metal ions (Fig. 2). The emission band at 416 nm was attributed to the enol form and the emission at 529 nm was assigned to the keto tautomer, produced by the ESIPT process (Scheme 2) [31]. The presence of two bands enables the possibility of ratiometric analysis by comparing the ratio of intensities of two bands as a function of analyte concentration. It has advantageous over conventional monitoring at single wavelength, as the method is free from errors associated with receptor concentration, photo bleaching and environmental effects [32]. When biologically important metal ions were added, no detectable fluorescence changes were observed (Fig. S6). Interestingly, addition of Zn<sup>2+</sup> to the solution of TZNP caused a marked fluorescence enhancement (Φ = 0.32), with the increase in intensity of emission band at

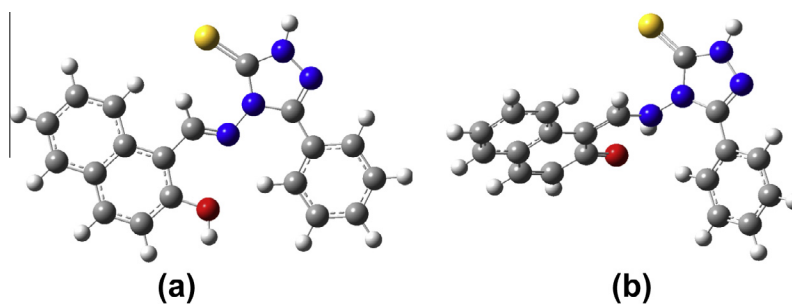


Fig. 6. Optimised structure of (A) enol and (B) keto form of TZNP.

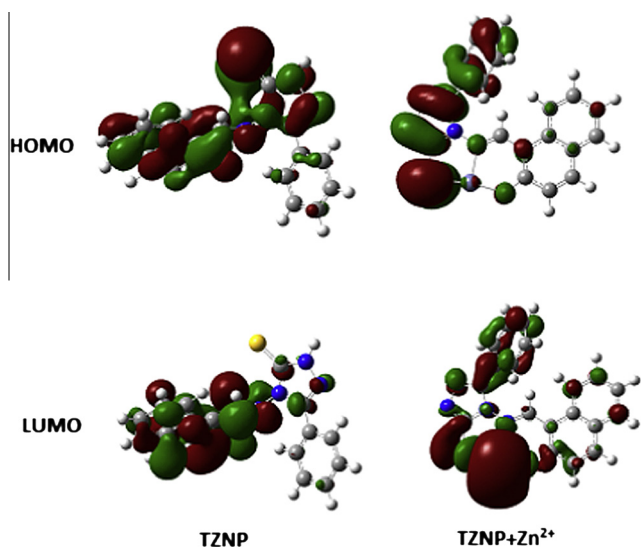


Fig. 7. Frontier molecular orbitals optimized at the B3LYP/LANL2DZ(d) level of theory.

529 nm along with concomitant decrease of the band at 416 nm, thus allowing rapid quantification of  $Zn^{2+}$  based on intensity ratio of enol and keto tautomer (Fig. 2).

From fluorescence titration [33], the binding constant of TZNP with  $Zn^{2+}$  was calculated to be  $3.25 \times 10^4 M^{-1}$ . When the ratiometric

intensity change  $I_{529}/I_{416}$  was plotted against  $[Zn^{2+}]$ , linearity was observed, which paves the way for quantitative determination of concentration of  $Zn^{2+}$  (Fig. S7). The detection limit was calculated from titration results and was found to be  $4.2 \times 10^{-7} M$  [34], which substantiates potential applications of TZNP in biological systems. To examine the reversibility of TZNP, the interaction of  $Zn^{2+}$ -TZNP complex with EDTA is studied. The addition of EDTA quenches the fluorescence of TZNP- $Zn^{2+}$  complex, indicating that TZNP acts as reversible chemosensor. It is noted that the fluorescence intensity upon addition of EDTA decreases with time and reaches a plateau within 2 min (Fig. S8).

The effect of pH on the probe was tested by recording fluorescence spectra over different pH values (Fig. S9). The fluorescence emission intensity of the probe is unaffected by pH values in the range of 4.5–8. At low pH range, protonation of probe disrupts the ESIPT process so that higher energy emission band assigned to the enol tautomer at 416 nm increases and no changes were observed at 529 nm. However in high pH range, fluorescence intensity at 416 nm increases due to deprotonation of phenolic hydroxyl group which otherwise causes non-radiative decay from the excited state by vibrationally coupling the excited state to water [35]. This process also disrupts the ESIPT phenomena and hence low energy band remain unaltered. Fluorescence intensity remains weak at intermediate pH (HEPES buffer (20 mM, pH 7.4). This observation clearly supported the involvement of phenolic group of probe in ESIPT phenomena.

To test the selective recognizing ability of TZNP, competitive experiments were performed in the presence of varying

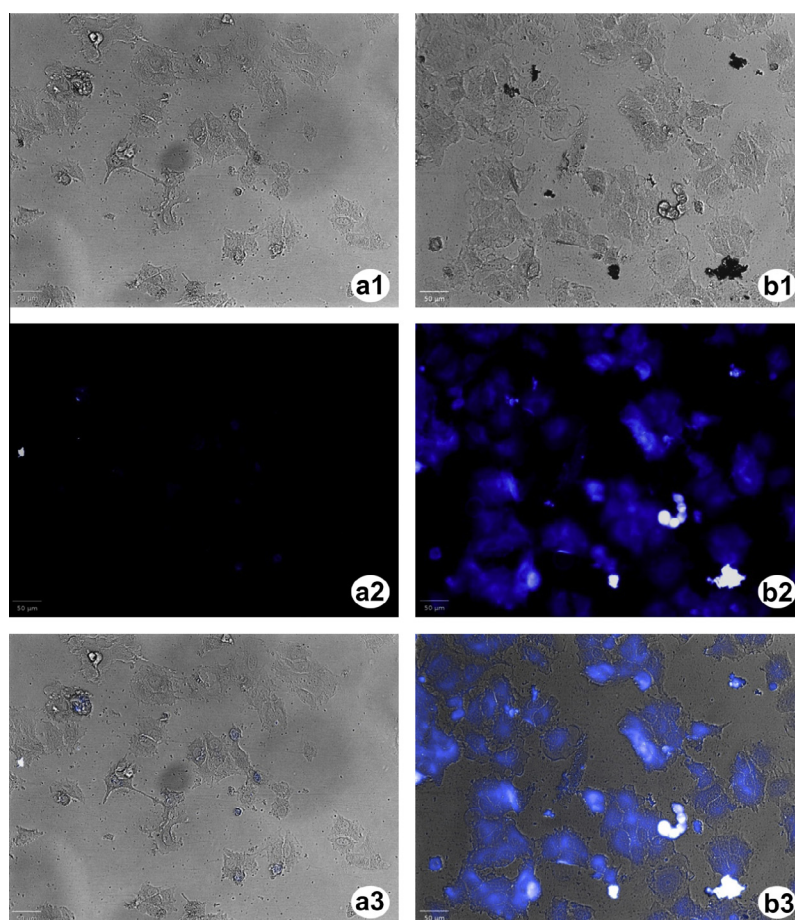


Fig. 8. (a) Intracellular localization of TZNP (10  $\mu M$ ) in MCF-7 cells. (b) Intracellular localization of the ability of TZNP for  $Zn^{2+}$  recognition in MCF-7 cells; (a1 and b1) Bright-field images; (a2 and b2) Florescent images; (a3 and b3) Bright-field and florescent superimposed image.

concentration of  $Zn^{2+}$  (0–20  $\mu M$ ), treated with 100  $\mu M$  of representative ions such as  $Na^+$ ,  $K^+$ ,  $Ca^{2+}$ ,  $Mg^{2+}$ ,  $Cu^{2+}$ ,  $Co^{2+}$ ,  $Ni^{2+}$ ,  $Fe^{2+}$ ,  $Fe^{3+}$ ,  $Hg^{2+}$ ,  $Cr^{3+}$ ,  $Pb^{2+}$ ,  $Mn^{2+}$ ,  $Ag^+$  and  $Cd^{2+}$  ions. No significant variation was observed in the presence of other competitive metal ions in comparison to solution containing only  $Zn^{2+}$  (Fig. 3). These results suggest that TZNP is capable of operating in a competing environment and thereby proves its robustness as ratiometric chemosensor for  $Zn^{2+}$ .

The stoichiometry of TZNP- $Zn^{2+}$  complex was evaluated by Job's plot using fluorometric titrations. Here the total concentration of TZNP and  $Zn^{2+}$  was kept constant in (DMSO/ $H_2O$ ) system, with continuously varying mole fraction of  $Zn^{2+}$  ion. The emission reached a maximum at 0.5 mol fraction of  $Zn^{2+}$ , thus indicating 1:1 binding stoichiometry of the complex formed between TZNP and  $Zn^{2+}$  ion (Fig. 4).

To further elucidate the binding properties of TZNP with  $Zn^{2+}$ ,  $^1H$  NMR spectra of TZNP before and after addition of  $Zn^{2+}$  was tested in DMSO- $d_6$  solution (Fig. 5). Upon addition of 0.5 eq of  $Zn^{2+}$  ion, the signals of aromatic ring proton became broad and got shifted downfield. At the same time, the proton signal of O-H group and CH=N at 10.4 ppm and 9.4 ppm shifted downfield and phenolic proton eventually disappeared with the addition of 1 eq of  $Zn^{2+}$ . Furthermore compared to addition of 1 eq of  $Zn^{2+}$ , no appreciable changes in  $^1H$  NMR spectra were observed upon addition of 1.5 eq of  $Zn^{2+}$ . Therefore, it appears that nitrogen atom of imine group, oxygen atom of hydroxyl group and sulphur atom plays a crucial role in efficient binding of TZNP with  $Zn^{2+}$ . To provide further support to the efficient binding of TZNP with  $Zn^{2+}$ , ESI-MS spectral studies were performed. The ESI-MS study, (Figs. S3 and S4), shows that peaks at  $m/z$  347.17 and  $m/z$  410.5 corresponds to  $[TZNP + H]^+$  and  $[(TZNP-2H)+Zn^{2+}+H]^+$  respectively, which corroborates 1:1 binding ratio for TZNP and  $Zn^{2+}$ . All these observations assure that the chemosensor TZNP bind selectively with  $Zn^{2+}$  metal ion.

To gain insight into the fluorescence enhancement of TZNP after  $Zn^{2+}$  binding, DFT calculations were performed for TZNP and TZNP- $Zn^{2+}$  using DFT/B3LYP - 6-31G basis set [36]. The optimized structure of enol and keto form of TZNP is shown in Fig. 6. In TZNP, the bond length between Zn and oxygen atom is 1.84 Å. Similarly, bond length of Zn and N is 1.97 Å and Zn-S bond length is 2.25 Å. Binding of  $Zn^{2+}$  to TZNP leads to the lowering of HOMO-LUMO energy gap, which might contribute to the appearance of absorption band around 417 nm. Evidently it is clear that triazole ring connected to hydroxynaphthaldehyde has a HOMO character while hydroxynaphthaldehyde along with nitrogen behaves as LUMO. Upon introduction of  $Zn^{2+}$ , HOMO of  $Zn^{2+}$  is shifted to benzotriazole moiety, while the LUMO are distributed over the phenolic ring of triazole with metal center and this could be the intrinsic factor for the fluorescence enhancement of TZNP after the addition of  $Zn^{2+}$  (Fig. 7).

Owing to its sensitivity, TZNP might be ideally suitable for intracellular  $Zn^{2+}$  imaging in living cells. At first, MCF-7 cells were incubated with probe TZNP alone and were subjected to fluorescence measurements. The cells were supplemented with  $Zn^{2+}$  for 24 h. A very weak intracellular fluorescence was observed in MCF-7 cells treated with TZNP. Interestingly, enhanced intracellular fluorescence was observed in MCF-7 cells treated with TZNP- $Zn^{2+}$  (Fig. 8). After treatment with TZNP- $Zn^{2+}$ , fluorescence and bright-field measurements made on MCF-7 cells confirmed that these cells were viable throughout the imaging experiments. In addition, cytotoxic property of probe was evaluated towards MCF-7 cells by MTT assay. The cancer cell lines were exposed to different concentrations of probe for 24 h and its corresponding  $IC_{50}$  value was found to be  $29.71 \pm 1.49 \mu M$  (Fig. S10). These experiments prove that TZNP shows good cell-permeability and biocom-

patibility. Thus TZNP can be successfully applied for intracellular sensing and imaging of  $Zn^{2+}$ .

## Conclusion

In summary, we have developed a triazole appended hydroxynaphthaldehyde unit (TZNP) that acts as a ratiometric fluorescent chemosensor for  $Zn^{2+}$  based on ESIPT mechanism. The probe senses  $Zn^{2+}$  ion with high sensitivity and excellent selectivity. The microscopic investigation revealed that TZNP has good cell-permeability and viable for imaging intracellular  $Zn^{2+}$  within living cells. It is expected that this  $Zn^{2+}$  selective sensor may find application in biomedical diagnostics and environmental detection.

## Acknowledgements

M.I., D.J. and K.K. thank UGC-BSR for research fellowship. M.I., D.J., K.K. and D.C. also acknowledge DST-IRHPA, FIST and PURSE for instrumental facilities. The authors gratefully acknowledge DBT-IPLS, School of Biological Sciences, MKU for providing instrumentation facilities.

## Appendix A. Supplementary material

Supplementary data associated with this article can be found, in the online version, at <http://dx.doi.org/10.1016/j.saa.2013.09.107>.

## References

- [1] R.A. Colvin, C.P. Fontaine, M. Laskowski, D. Thomas, *Eur. J. Pharmacol.* 479 (2003) 171–185.
- [2] J. Berg, Y. Shi, *Science* 271 (1996) 1081–1085.
- [3] D.W. Choi, J.Y. Koh, *Annu. Rev. Neurosci.* 21 (1998) 347–375.
- [4] A.I. Bush, *Trends Neurosci.* 26 (2003) 207–214.
- [5] Z. Liu, W. He, Z. Guo, *Chem. Soc. Rev.* 42 (2013) 1568–1600.
- [6] K. Sreenath, R.J. Clark, L. Zhu, *J. Org. Chem.* 77 (2012) 8268–8279.
- [7] M. Natali, L. Soldi, S. Giordani, *Tetrahedron* 66 (2010) 7612–7617.
- [8] Z.L. Gong, B.X. Zhao, W.Y. Liu, H.S. Lv, *J. Photochem. Photobiol. A* 218 (2011) 6–10.
- [9] L.E. McQuade, S.J. Lippard, *Inorg. Chem.* 49 (2010) 9535–9545.
- [10] S.A. Ingale, F. Seela, *J. Org. Chem.* 77 (2012) 9352–9356.
- [11] A. Misra, M. Shahid, P. Srivastava, *Sensors Actuat., B* 169 (2012) 327–340.
- [12] G.Q. Zhang, G.Q. Yang, L.N. Zhu, Q.Q. Chen, *Sensors Actuat., B* 114 (2006) 995–1000.
- [13] M. Li, H.Y. Lu, R.L. Liu, J.D. Chen, C.F. Chen, *J. Org. Chem.* 77 (2012) 3670–3673.
- [14] C. Gao, X. Jin, X. Yan, X. Yao, Y. Tang, *Sensors Actuat., B* 176 (2013) 775–781.
- [15] F. Xiao, J. Shen, J. Qu, S. Jing, *Inorg. Chem. Commun.* 35 (2013) 69–71.
- [16] L.Y. Zhao, Q.L. Mi, G.K. Wang, J.H. Chen, J.F. Zhang, Q.H. Zhao, Y. Zhou, *Tetrahedron Lett.* 54 (2013) 3353–3358.
- [17] T. Lijima, A. Momotake, Y. Shinohara, T. Sato, Y. Nishimura, T. Arai, *J. Phys. Chem. A* 114 (2010) 1603–1609.
- [18] D.A. Yushchenko, V.V. Shvadchak, A.S. Klymchenko, G. Duportail, V.G. Pivovarenko, Y. Mely, *J. Phys. Chem. A* 111 (2007) 10435–10438.
- [19] J. Zhao, S. Ji, Y. Chen, H. Guo, P. Yang, *Phys. Chem. Chem. Phys.* 14 (2012) 8803–8817.
- [20] K. Mulla, P. Dongare, D.W. Thompson, Y. Zhao, *Org. Biomol. Chem.* 10 (2012) 2542–2544.
- [21] H.A. Zamani, H. Behmadi, E.-J. Chem. 9 (1) (2012) 308–312.
- [22] S.B. Revin, S.A. John, *Sensors Actuat., B* 161 (2012) 1059–1066.
- [23] N. Chidananda, B. Poojary, V. Sumangala, N. Suchetha Kumari, P. Shetty, T. Arulmoli, *Eur. J. Med. Chem.* 51 (2012) 124–136.
- [24] G. Sivaraman, T. Anand, D. Chellappa, *Analyst* 137 (2012) 5881–5884.
- [25] G. Sivaraman, T. Anand, D. Chellappa, *RSC Adv.* 2 (2012) 10605–10609.
- [26] G. Sivaraman, D. Chellappa, *J. Mater. Chem. B* 1 (2013) 5768–5772.
- [27] G. Sivaraman, V. Sathiyaraja, D. Chellappa, *J. Lumin.* 145 (2014) 480–485.
- [28] G. Sivaraman, T. Anand, D. Chellappa, *RSC Adv.* 3 (2013) 17029–17033.
- [29] A.S. Shawali, E.S. Darwish, F.M. A Altalbawy, *Asian. J. Spectrosc.* 12 (2008) 113–120.
- [30] S. Goel, O.P. Pandey, S.K. Sengupta, *Bull. Soc. Chim. Fr.* (1989) 771.
- [31] W.R. Cordoba, C. Fregoso, E. Zuzogagoitia, J. Peon, *J. Phys. Chem. A* 111 (2007) 6241–6247.
- [32] S. Banthia, A. Samanta, *J. Phys. Chem. B* 110 (2006) 6437–6440.
- [33] K.A. Connors, *Binding Constants*, Wiley, New York, 1987.
- [34] M. Shortreed, R. Kopelman, M. Kuhn, B. Hoyland, *Anal. Chem.* 68 (1996) 1414.
- [35] J.F. Callan, A.P. de Silva, D.C. Magri, *Tetrahedron* 61 (2005) 8551–8588.
- [36] Gaussian 03, Revision C.02, M.J. Frisch, G. Trucks, H.B. Schlegel, G.E. Scuseria, M.A. Robb, J.R. Cheeseman, J.A. Montgomery, T. Vreven, K.N. Kudin, J.C. Burant,

J.M. Millam, S.S. Iyengar, J. Tomasi, V. Barone, B. Mennucci, M. Cossi, G. Scalmani, N. Rega, G.A. Petersson, H. Nakatsuji, M. Hada, M. Ehara, K. Toyota, R. Fukuda, J. Hasegawa, M. Ishida, T. Nakajima, Y. Honda, O. Kitao, H. Nakai, M. Klene, X. Li, J.E. Knox, H.P. Hratchian, J.B. Cross, V. Bakken, C. Adamo, J. Jaramillo, R. Gomperts, R.E. Stratmann, O. Yazyev, A.J. Austin, R. Cammi, C. Pomelli, J.W. Ochterski, P.Y. Ayala, K. Morokuma, G.A. Voth, P. Salvador, J.J.

Dannenberg, V.G. Zakrzewski, S. Dapprich, A.D. Daniels, M.C. Strain, O. Farkas, D.K. Malick, A.D. Rabuck, K. Raghavachari, J.B. Foresman, J.V. Ortiz, Q. Cui, A.G. Baboul, S. Clifford, J. Cioslowski, B.B. Stefanov, G. Liu, A. Liashenko, P. Piskorz, I. Komaromi, R.L. Martin, D.J. Fox, T. Keith, M.A. AlLaham, C.Y. Peng, A. Nanayakkara, M. Challacombe, P.M.W. Gill, B. Johnson, W. Chen, M.W. Wong, C. Gonzalez, J.A. Pople, Gaussian Inc., Wallingford, CT, 2004.